



The beginning heights and light curves of high-altitude meteors

Pavel KOTEN^{1*}, Pavel SPURNÝ¹, Jiří BOROVIČKA¹, Stephen EVANS², Andrew ELLIOTT²,
Hans BETLEM³, Rostislav ŠTORK¹, and Klaas JOBSE³

¹Astronomical Institute of Academy of Sciences, Ondřejov Observatory, 251 65 Ondřejov, Czech Republic

²British Astronomical Association, Burlington House, Piccadilly, London W1J 0DU, United Kingdom

³Dutch Meteor Society, Lederkarper 4, 2318 NB Leiden, The Netherlands

*Corresponding author. E-mail: koten@asu.cas.cz

(Received 15 May 2005; revision accepted 30 June 2006)

Abstract—In this paper, we provide an overview of meteors with high beginning height. During the recent Leonid meteor storms, as well as within the regular double station video observations of other meteor showers, we recorded 164 meteors with a beginning height above 130 km. We found that beginning heights between 130 and 150 km are quite usual, especially for the Leonid meteor shower. Conversely, meteors with beginning heights above 160 km are very rare even among Leonids. From the meteor light curves, we are able to distinguish two different processes that govern radiation of the meteors at different altitudes. Light curves vary greatly above 130 km and exhibit sudden changes in meteor brightness. Sputtering from the meteoroid surface is the dominating process during this phase of the meteor luminous trajectory. Around 130 km, the process switches to ablation and the light curves become similar to the light curves of standard meteors. The sputtering model was successfully applied to explain the difference in the beginning heights of high-altitude Leonid and Perseid meteors. We show also that this process in connection with high altitude fragmentation could explain the anomalously high beginning heights of several relatively faint meteors.

INTRODUCTION

The height range at which the meteor phenomenon occurs is related to the structure of a meteoroid and to its initial velocity and mass (e.g., Ceplecha 1968). Of special interest is the beginning height of the meteor. Until recently, the commonly held opinion was that meteor ablation usually starts below 130 km. The beginning heights of photographic meteors are between 70 and 120 km, depending on the initial velocity (Ceplecha 1968). Of the 4581 photographic meteors recorded in the IAU Meteor Data Center (Lindblad et al. 2003), the beginning heights of 4027 are given. Of these meteors, the beginning heights of just 22 are higher than 120 km, and in only five cases is the beginning height higher than 130 km. The average beginning height lies below 100 km. In addition, earlier double-station observations of meteors using more sensitive television cameras confirmed this opinion. In the studies of Hawkes et al. (1984) and Sarma and Jones (1985), only a few meteors with beginning heights above 120 km were found, and none above 130 km were found.

Ueda and Fujiwara (1995) reported orbits of 326 meteors that were determined on the basis of television observations.

They did not provide beginning height analyses, but in Table 1 it is clear that the beginning heights of just 18 meteors are higher than 120 km and only two are higher than 130 km. The maximum beginning height is only 131 km, despite the fact that the television technique is generally more sensitive in comparison with the photographic observations.

Woodworth and Hawkes (1996) mentioned that the relatively small field of view of the typical video or television camera as well as the optimum intersection of these observations at about 95 km results in a bias against higher meteors. They improved the observational technique, which resulted in a relatively smaller bias against higher meteors, but found the lack of meteors above 120 km seemed to be a real effect. Despite the better sensitivity of the cameras used (about magnitude +9.5) and the optimal intersection between 115 and 125 km, they did not detect any meteors with higher beginning height.

Multi-station television and photographic observation concentrating on bright Leonid meteors were carried out in Japan in November 1995 and 1996. Fujiwara et al. (1998) reported two bright Leonid meteors observed using both techniques. The photographic beginning heights of both meteors are below 130 km. However, the television cameras

Table 1. The numbers and beginning heights of the meteors with a beginning height above 130 km in different meteor showers. The total number of such cases is given in the second column; other columns show the numbers of meteors with the beginning height in different height intervals.

	Number of cases	130–150 km	150–160 km	>160 km
Leonids 1998	18	5	4	9
Leonids 1999	11	10	0	1
Leonids 2000	17	15	0	2
Leonids 2001	102	101	0	1
Perseids	9	8	0	1
Lyrids	1	1	0	0
η -Aquadrids	2	1	1	0
Sporadic	4	4	0	0

recorded the beginnings of both meteors at about 160 km. The authors suggested different limiting magnitude as well as different spectral sensitivity as the primary reasons for this difference. They also concluded that the beginning height of the high-velocity meteors could be much higher than was previously thought.

This idea was quickly confirmed during several years of enhanced activity of the Leonid meteor stream in the late 1990s and early 2000s. As a part of the 1998 Leonid multi-instrument aircraft campaign (Jenniskens and Buttow 1999), a ground-based international expedition to China photographically recorded several tens of fireballs with the beginning height up to 130 km during the so-called “fireball night” on November 16 and 17. Some of these were also recorded using an all-sky video camera. The beginning heights of 12 of these meteors were several tens of kilometers higher, with the maximum beginning height at 199 km (Spurný et al. 2000a). Moreover, as shown in Spurný et al. (2000b), the beginning heights of the meteors, which were also recorded by even more sensitive narrow field-of-view video cameras, are on average 18 km higher in comparison with the height determined from the all-sky video camera. The brightest, which reached photographic maximum brightness of magnitude -12.5 , started on this video record at 195 km. Because the highest meteors detected by the video all-sky camera meteor started at 199 km, it is evident that the real beginning height of at least this case should be above 200 km. Furthermore, these meteors showed unusual behavior at heights above 130 km. For several cases, a comet-like diffuse appearance is reported. Unusual structures extending several kilometers sideways from the brightest part of meteor were observed. When these meteors reached an altitude of 130 km, their appearance quickly changed to the typically observed drop-like shape (Spurný et al. 2000b).

Another case of a high-altitude fireball was observed during the 1999 Leonid MAC mission. A very bright fireball (magnitude -13 at maximum) was recorded by several spectrographs. Jenniskens and Rairden (2000) described the

evolution of its persistent train, provided its triangulation, and by extrapolation estimated that the beginning height of the fireball was about 195 km. Independent trajectory evaluation by Borovička and Jenniskens (2000) confirmed this beginning height. The diffuse phase continued down to about 136 km. Murray et al. (1999) also reported a case of an unusual Leonid meteor with a nebulous appearance. Despite the single-station observation, they estimated that the beginning height of this meteor was about 138 km. Later, the meteor reached maximum brightness of magnitude -4 . The ejected material was observed at an average distance of 450 m from the main body. Another case of transverse spread in a Leonid meteor was described in the paper of LeBlanc et al. (2000). Light production was observed in the region of about 600 m perpendicular to the flight direction of the meteor. On the other hand, the trail widths of the standard meteors are thought to be up to a few tens of meters (Campbell-Brown and Jones 2003).

It is not only the Leonid meteor shower that produces meteors with a higher beginning height. Koten et al. (2001) reported observations of one Lyrid, two η -Aquadrid, and one Perseid meteor with beginning heights above 130 km.

Other teams also observed the recent Leonid meteor storms. On the basis of 79 double-station Leonid meteors, Campbell et al. (2000) reported that the beginning heights of the vast majority of the meteors lie in the interval between 100 and 120 km. The highest beginning height was 144.3 km observed on November 16, 1998. Similar results also were obtained for the 1999 Leonid shower. Brown et al. (2002a) found that the beginning height of the meteors has a Gaussian distribution with an average height of 123.3 km and width of 7.8 km. Despite the fact that some meteors with beginning heights above 140 km were observed, the relative lack of higher beginning heights (above 160 km) was again experienced. Meteoroid masses between 10^{-8} and 10^{-4} kg were reported in this paper. During the 2002 Leonid meteor storm, Gährken and Michelberger (2003) observed a Leonid meteor with a beginning height of at least 165 km. The most probable value is 174 ± 8 km. They reported the diffuse structure at higher altitudes.

Classical ablation theory, which assumes that intensive vaporization is responsible for meteor radiation, cannot explain meteor luminosity above 130 km. The atmospheric mean free path is from several tens up to few hundreds meters at altitudes between 160 and 200 km. The meteoroid body is too cold to produce light in classic way. Another explanation of this phenomenon has therefore been sought. Brosch et al. (2001) considered a simple sputtering model as an explanation of the meteor trails observed by radar at high altitudes. Hill et al. (2004) modeled meteor light curves contributed by both the sputtering process and the thermal ablation. They found very good agreement with the light curves observed by Fujiwara et al. (1998) and Spurný et al. (2000a, 2000b). Rogers et al. (2005) compared meteoroid mass loss due to sputtering and thermal processes and found

that in some cases the sputtering from meteoroid bodies is very important. In the case of relatively small and very fast particles, the sputtering can contribute up to around 80% of the total mass lost during the atmospheric flight. As it is shown later in this paper, the high-altitude meteors are produced by meteoroids with masses higher than 10^{-4} kg. For such meteors, Rogers et al. (2005) found that the sputtering could contribute to about 10% of the total mass loss. Nevertheless, it is necessary to note that these numbers are not exact because there are several other factors that could influence total contribution of the sputtering. Popova et al. (Forthcoming) showed that the sputtering is essential for high-velocity meteors and negligible for meteor velocities below 30 km/s. Vinkovic (Forthcoming) showed that the high-altitude meteor phenomenon can be explained by the sputtering. He found that the particle sputtered from the meteoroid surface needs between 100 and 200 collisions to be slowed down to the thermal level of surrounding atmosphere. A cascade of such collisions is sufficient to produce enough light for detection by video cameras. Moreover, Monte Carlo model images of meteors coincide with observed shapes and sizes of high altitude meteors.

SUMMARY OF HIGH-BEGINNING-HEIGHT METEORS

In this paper, we provide an overview of all cases of meteors that were observed above 130 km within all our observational programs. This means that some of the above-mentioned meteors are also included in this study. For the purpose of this paper, all meteors with beginning heights below 130 km are called “standard” meteors, whereas those radiating above 130 km are “high-altitude” meteors. This threshold was chosen because until recently, meteors were observed only below this altitude and the classical ablation theory cannot explain meteor radiation at higher altitudes.

The overall number of meteors radiating above 130 km in our sample is 164 events. 145 of these events, or about 90%, are Leonids. Of the others, nine are Perseids, two are η -Aquarids, and one is a Lyrid. Four cases are sporadic meteors. A summary of all of the cases is given in Table 1. Despite the fact that we detected a total of 164 high-altitude meteors, this number is still only around 5% of all double-station video meteors that were detected within all our observation programs. A quick look at the velocity distribution of these meteors shows that higher velocities are preferred. Leonid, η -Aquarid, Perseid and all sporadic meteors have an initial velocity above 54 km/s. The only exception is the Lyrid meteor, with an initial velocity of 46.5 km/s. Conversely, Orionid meteors above 130 km were not detected despite the fact that this shower belongs among those with high initial velocity.

At this point, we should comment on the exceptional position of the 2001 Leonid data in the whole sample of the

high-altitude meteors. Comparison of the observed 1767 filament encounter with results from previous years of high Leonid activity shows there was an excess of bright meteors in 2001. During the 1998 (at just the time of predicted maximum and not including the “fireball night”), 1999, and 2000 observations, rather fainter meteors were recorded. Moreover we gained a lot of experience during previous campaigns and the experiment in 2001 was more suitable for the observation of high-altitude meteors. More cameras were used, their fields of view were overlapped, and the intersection point for double station observation was higher in the atmosphere in comparison with previous years. The result of this better strategy was not only higher numbers of the high-altitude meteors, but also the light curves of a higher number of the meteors were completely covered. It is only possible to speculate on what data would have been recorded by carrying out such an experiment during the “fireball night” in 1998.

OBSERVATIONS AND INSTRUMENTATION

All reported meteors were observed within our double-station meteor observation program using video techniques, either in the Czech Republic or during special expeditions dedicated to the Leonid meteor storms. Several types of cameras contributed this work. The Czech cameras usually consisted of an Arsat 1.4/50 mm lens fitted to a Dedal-41 second-generation image intensifier and a Panasonic S-VHS commercial camcorder. In this configuration, the camera provides a field of view (FOV) with a diameter of about 25° (cameras A and B). The same system is additionally equipped with a spectral grating that is also used at the Ondřejov station and sometimes is able to detect a beginning of a high-altitude meteor in the zero order of the spectra (camera C). Another wide-field system with a Zenitar 2.8/16 mm lens providing a FOV of 80° is in operation at the Kunžak station (camera D). The same instrumentation was used also during all Leonid expeditions along with several other cameras. Stephen Evans operated a Sony Hi8 camcorder with a second-generation MPC image-intensifier and Canon FD 1.8/28 mm lens providing a FOV of 36° (camera E) and Andrew Elliott a similar camera with a FOV of 40° (camera F). Another system, consisting of a Sony Hi8 camcorder, Mullard XX1332 image intensifier and Canon FD 1.2/85 mm lens giving a FOV of $25 \times 35^\circ$, was operated by Klaas Jobse (camera G) during the 1998 Leonid expedition. The Leonid observational campaigns were usually covered by batteries of 35 mm photographic cameras of Hans Betlem (camera P). Several Leonid expeditions were also supported by all-sky photographic cameras with 35 mm fish-eye lenses. The same cameras regularly monitor the sky above the Czech Republic within the European fireball network (camera S) and provided valuable data on several meteors included in this work (Spurný et al 2004). The coordinates of the double-station

Table 2. The double-station experiments. Given for each station (Station 1 and Station 2 columns) are its name (first row), the geographical coordinates in the form of eastern longitude (second row), northern latitude (third row) and elevation above the sea level (fourth row), as well as camera equipment (fifth row). The capital letters in the fifth row are the same as mentioned in the text. The last column of the table provides information about the distance of both stations and the azimuth of the second station (south = 0°).

Experiment	Date	Country	Station 1	Station 2	Distance, azimuth
Regular double-station	April 1998 to date	Czech Republic	Ondřejov 14°46'48.8" 49°54'36.8" 524 m A, C, S	Kunžak 15°12'2.8" 49°6'27.2" 652 m B, D	94.3 km 341°
1998 Leonids	16–19 November 1998	China	Xinglong 117°34'27.5" 40°23'48.5" 960 m B, P, S	Lin Ting Kou 117°30'17" 39°37'47" 56 m G, P, S	85.4 km 4°
1999 Leonids	16–19 November 1999	Spain	Casa Nueva 357°16'39.8" 39°7'1.4" 795 m A, P, S	Punto Alto 356°58'1.98" 38°22'45.44" 788 m B, E, P, S	86.2 km 18.3°
2000 Leonids	17–19 November 2000	Spain	Curica 357°34'6.2" 37°51'26.6" 1007 m A, P	Lucainena 357°46'1.6" 37°02'13.7" 707 m B, C, E, P	92.7 km 349°
2001 Leonids	17–18 November 2001	Arizona, USA	Antelope Mesa 249°47'55.5" 35°47'57.7" 1975 m D, E, P	Crystal Forest 250°6'34.7" 34°47'34.8" 1664 m A, C, F, P	115.2 km 345.9°

experiment locations as well as the associated camera equipment are summarized in Table 2.

All records were stored on video tape in S-VHS or Hi8 format in PAL standard, which provides a time resolution of 0.04 s. The meteors were either searched for manually or by using the MetRec automatic detection software (Molau 1999) and then digitalized with a PC frame-grabber. Each frame was transformed into a 768×576 pixel, 8-bit monochrome image and stored in non-compressed AVI format. All meteors were measured by means of our original self-automatic software MetPho and their trajectories and orbits computed using standard procedures. Orbits were compared with the reference orbits of meteor showers (Cook 1973) using the so-called D criterion (Southworth and Hawkins 1963). The complete procedure is described in more detail in Koten (2002). Note that we are able to measure the meteor position on the image with precision of 0.2 pixels, which corresponds to an angular precision of about 0.5'. Each pixel covers an area of $150 \text{ m} \times 150 \text{ m}$ at the distance of 200 km and smaller at lower distances. On the other hand, it is difficult to precisely determine the location of the meteor during its diffuse phase. Thus, we set 1 km as the upper limit of the altitude determination error at this phase of the meteor. Below 130 km, where the meteors resemble drop-shaped objects, the precision of the height determination is much better. The height error is 0.1 km in this region.

BEGINNING HEIGHTS

The beginning height distribution of all meteors above 130 km is given in Fig. 1. The dominance of the Leonid meteors among high-altitude meteors is evident from this figure as well as from the fact that the beginning heights between 130 and 150 km are usual, particularly among meteors of this shower. Such meteors are less frequent among other meteor showers. Figure 2 shows a histogram of the beginning heights for only the Leonid meteors observed in 2001. Data on 396 meteors are used for this plot. When we look at this height distribution, we can see that there is no strict cut-off at 130 km. Transition of that level in the plot is quite smooth and there are still many meteors with beginning heights above 130 km. Their fraction represents approximately one-quarter of the total number of all Leonid meteors. Both Fig. 1 and Fig. 2 also show that beginning heights above 160 km are very rare, even among Leonid meteors. Such high beginning height was detected only for the brightest meteors. All these instances are Leonid meteors (13 cases); the only exception is the Perseid meteor with the beginning height just above this value (161 km). From this point of view, the “fireball night” of Leonid meteors that occurred in 1998 was exceptional and, despite the fact that we recorded more high-altitude meteors, such an event did not reoccur.

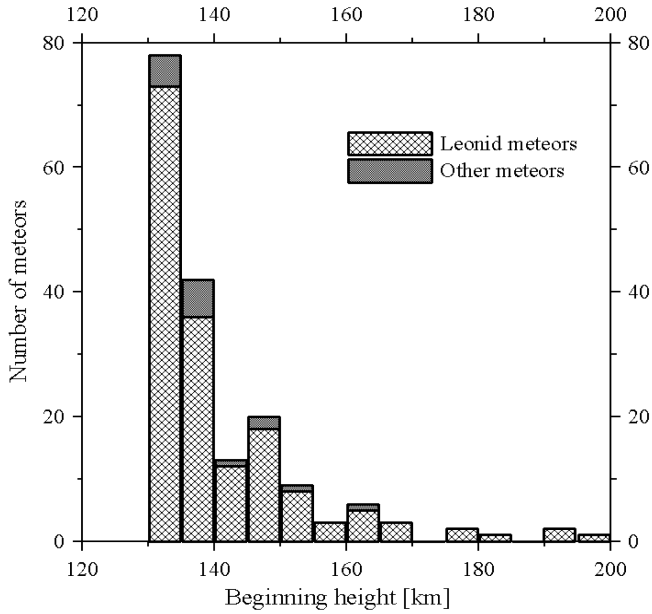


Fig. 1. A histogram showing the beginning heights of all 164 high-altitude meteors. 148 meteors are members of the Leonid meteor shower; 16 meteors belong to other showers or are sporadic.

This could be confirmed using another plot. Figure 3 shows the beginning heights of meteors as a function of their photometric mass. The photometric mass of the meteor is calculated by integration of its light curve using luminous efficiency according to Ceplecha (1988). Several meteors for which the photometric mass could not be computed precisely are included in the plot as well. The usual case is that such meteors left the field of view of our video cameras. We estimated their maximum brightness from the photographic records. Using the relationship between the maximum brightness and photometric mass (determined for each shower separately), probable value of the photometric mass was calculated. These meteors are plotted as solid lines at the relevant height level, which represent the range of photometric masses according to the error of the brightness estimate. Only for meteors recorded by the photographic fish-eye camera could our standard procedure of computing the mass from photographic data be employed. Meteors EN130801A and EN110800 are such cases. The first one was the highest non-Leonid (Perseid) meteor with a photometric mass of 600 g. More data on both meteors are available in Spurný et al. (2004). For the purpose of the following analyses, we use only meteors with complete light curves. Only exception are peculiar meteors discussed later.

Figure 3 shows that the beginning height H_{BEG} increases with increasing photometric mass m_p . This fact was previously reported for generally fainter meteors of several cometary meteor showers (Koten et al. 2004) and also for brighter meteors (Spurný et al. 2000a). According to the first paper, a slope of the dependence at a first approximation

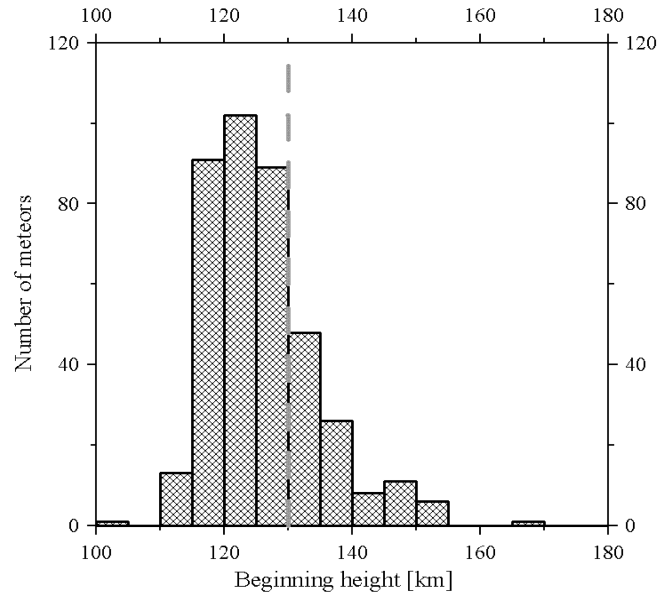


Fig. 2. The beginning heights of 396 Leonid meteors observed in 2001 are included in this plot. The meteors belong to the filament ejected from the parent comet in 1767. The dashed gray line represents a height of 130 km.

should be around 10. Using all meteors included in Fig. 3, we find the relationship:

$$H_{\text{BEG}} = 9.0 (\pm 0.3) * \log m_p + 145.4 (\pm 0.7) \quad (1)$$

where the value 9.0 is in good agreement with the theoretical one (Koten et al. 2004). Although the linear fit follows the behavior of the majority of the meteors, the brightest (and the highest) Leonids are plotted above it. Assuming only meteors with a beginning height above 150 km, the slope is steeper as shown by the dashed line in Fig. 3. The linear fit provides the value 11 ± 2 .

Because many authors present a maximum absolute brightness of the meteor M_{Max} rather than its mass, we provide also the equation for this quantity:

$$H_{\text{BEG}} = -3.5 (\pm 0.1) * M_{\text{Max}} + 124.4 (\pm 0.4) \quad (2)$$

The maximum brightness values stretch from +3.8 to -14.4 magnitudes in our data sample. Campbell et al. (2000) analyzed the observations of the 1998 Leonid meteor shower and found the following relationship:

$$H_{\text{BEG}} = -3.0 (\pm 0.4) * M_{\text{Max}} + 123.9 (\pm 1.7) \quad (3)$$

Both results are similar, despite the fact that the second sample contains rather fainter meteors with the maximum brightness between 0 and +6 magnitudes. This means that both faint and bright Leonid meteor follow a similar dependence of the beginning height on the maximum brightness (or the photometric mass). Assuming the sputtering at high altitudes Vinkovic (Forthcoming) derived the dependence of the beginning height H_{BEG} on the

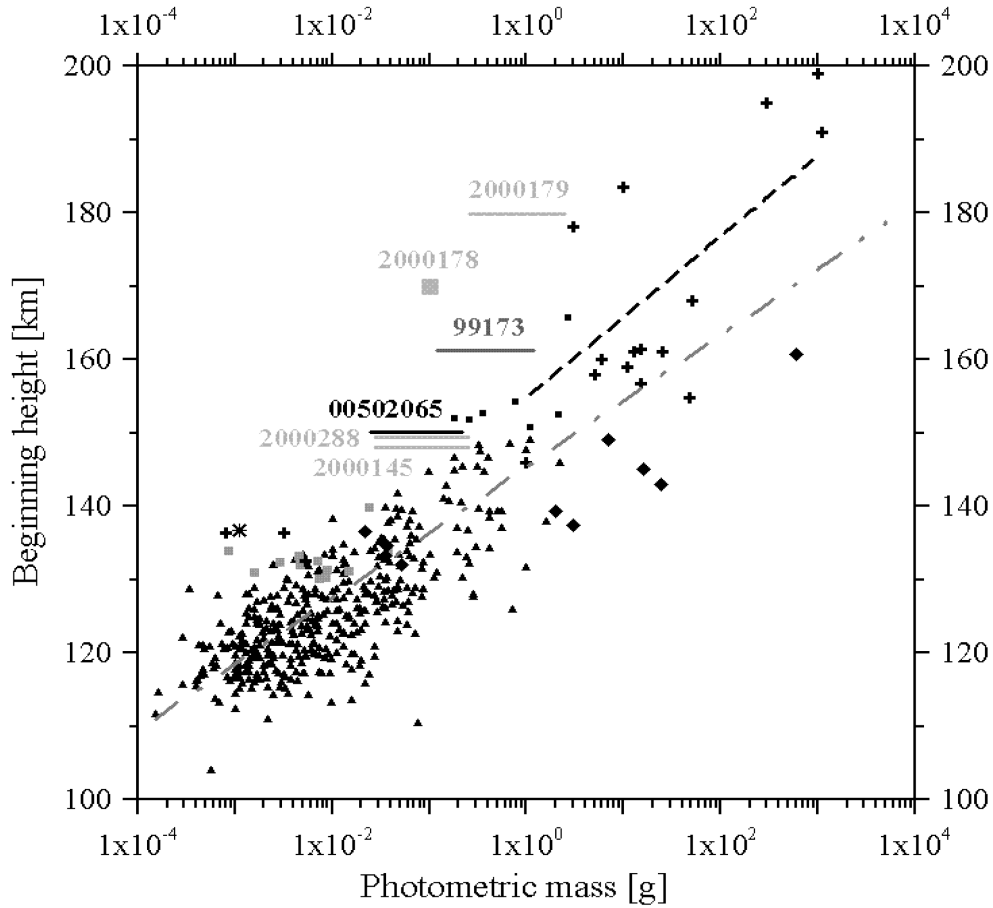


Fig. 3. The beginning height as a function of photometric mass. Triangles represent 2001 Leonid meteors. The Leonid meteors observed in 1998 are plotted as crosses (adopted from Spurný et al. 2000a, 2000b), the 2000 Leonid meteors as gray squares, and Perseid and sporadic meteors as black diamonds. The asterisk represents the Lyrid meteor. The solid lines show the probable ranges of the photometric masses of meteors, for which this value is not possible to compute directly. Note that except for Leonids 2001, only meteors with beginning heights above 130 km are included in the plot. The dot-and-dashed gray line represents a linear fit on all data, whereas the dashed black line represents a fit only on the meteors with beginning height above 150 km.

meteoroid size and applied it successfully on the observations of Campbell et al. (2000) and Spurný et al. (2000a). Our additional data are in good agreement with this evaluation and fit the gap between both presented data sets of faint and very bright meteors, respectively.

Equation 3 shows that the beginning height is higher for brighter meteors. In the single body approximation the maximum brightness of the meteor depends on its mass according to the following relationship (for derivation, see, e.g., Appendix in Vinkovic, Forthcoming):

$$M_{\text{Max}} = -2.5 * \log m_p - 2.5 * \log \cos Z + \text{constant} \quad (4)$$

where Z is the zenith distance of the meteor radiant. Again, for all meteors included in Fig. 3, we derive the relationship between the maximum brightness M_{Max} , the photometric mass m_p (in kg) and the zenith distance Z of the meteor:

$$M_{\text{Max}} = -2.47 (\pm 0.02) * \log m_p - 1.02 (\pm 0.13) * \log \cos Z - 12.34 (\pm 0.13) \quad (5)$$

In comparison with the theoretically derived Equation 4 this relationship shows the same dependence of the maximum brightness on the photometric mass and weaker dependence on the zenith distance of radiant. Our results are comparable with observations of the 1998 Leonids by Campbell et al. (2000):

$$M_{\text{Max}} = -1.89 (\pm 0.07) * \log m_p - 1.35 (\pm 0.63) * \log \cos Z - 8.76 (\pm 0.46) \quad (6)$$

and 1999 Leonids by Brown et al. (2002a)

$$M_{\text{Max}} = -2.14 (\pm 0.12) * \log m_p - 0.04 (\pm 2.40) * \log \cos Z - 11.56 (\pm 0.13) \quad (7)$$

Equations 6 and 7 cover a significantly narrower range of the values of the maximum brightness. Although the coefficients vary slightly, all these equations follow the same general trend. Thus we confirm the relationship between the beginning height of meteor and its size on the sample of significantly higher number of meteors covering a much

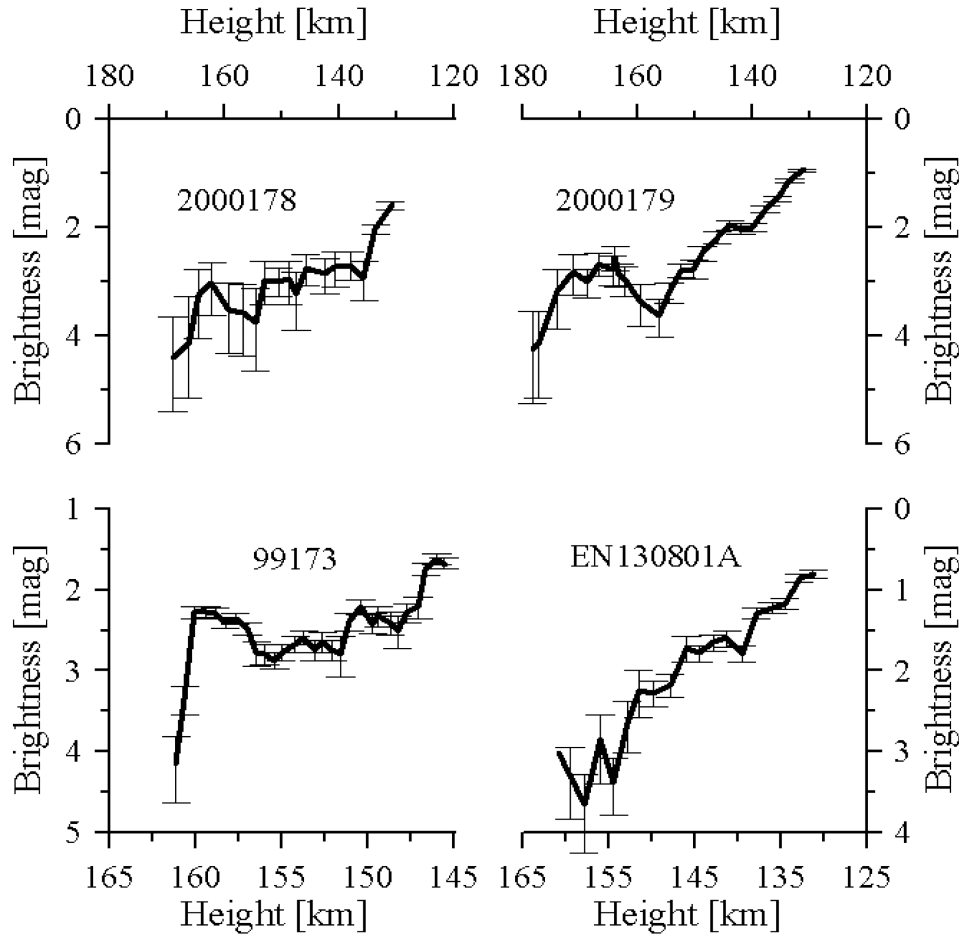


Fig. 4. Light curves of the high-altitude meteors. Only parts above 130 km for the meteors 2000178 (top left), 2000179 (top right), 99173 (bottom left) and EN130801A (bottom right) are plotted. Meteor 99173 left the field of view even higher, at 145 km. The absolute brightness (recomputed to the 100 km distance) is used on the y-axis. The error box is given for each measured point.

broader range of sizes (masses) than previously published data.

The beginning height steadily increases up to the altitude 150–160 km regardless as to whether classical ablation (for standard meteors) or sputtering (for high altitude meteors) is presumed to be responsible for the light production. No exceptionality to the 130 km altitude is visible. The mass threshold for 130 km is around 10^{-4} kg. Leonid meteors with higher photometric mass usually start their luminous trajectory above 130 km, though there is a significant scatter of beginning heights for any given mass. Above ~ 150 km, the beginning height of the Leonids is even higher than this relationship predicts. It could suggest that the sputtering process is more efficient here than the thermal ablation below 130 km, i.e., one impinging molecule produces more light because it starts the cascade of many collisions.

The Perseids and the sporadic meteors with masses greater than 1 g have lower beginning heights in comparison with the Leonids of similar masses. Different entry velocities of the showers can explain this variance. The sputtered atoms

have about 5–10% of the incoming energy (Field et al. 1997). If the kinetic energy of the colliding molecule is smaller, the particle sputtered from the meteoroid body has lower energy, too. Consequently, the total number of emitted electrons in one cascade γ necessary to slow down the sputtered particles to the thermal level of the atmosphere is also smaller. According to the different kinetic energy of incoming particle, we assume that $\gamma_p = 0.7 \gamma_L$, where γ_p and γ_L are the values for the Perseids and the Leonids, respectively. Moreover, the sputtering yield Y , which is defined as the number of sputtered particles relative to the number of projectiles, depends besides other properties, on the projectile velocity. According to Popova et al. (Forthcoming), Y could be approximately two times higher for Leonid than Perseid meteors. Using the equation for the apparent meteor magnitude M (Vinkovic, Forthcoming):

$$M = -1^m - 2.5 \log \left(\frac{\gamma Y R_m^2 v_m n_{\text{atm}} \Psi E_0}{4 D^2 F_{\text{Sirius}}} \right) \quad (8)$$

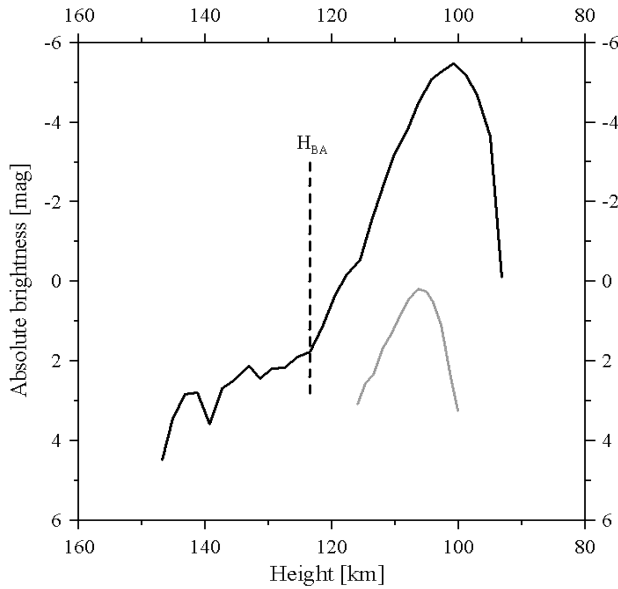


Fig. 5. The plot provides comparison of two cases of meteors. Meteor 20010467 (full black line) is a typical case of the high-altitude meteors with the beginning height at 147.6 km. The dashed vertical line shows the beginning of the ablation phase of the light curve (H_{BA}). The fluctuations on the light curve are visible above 130 km. The light curve is smooth below this altitude. On the other hand meteor 20010209 (gray line) is representative of the standard meteors.

where R_m is the radius of the meteoroid, v_m is the meteor velocity, n_{atm} is the atmospheric number density, Ψ is the fraction of photons contributing to the flux measured in one pixel, E_0 is the energy of photon, D is the distance of the meteor, and F_{Sirius} is the flux of Sirius, we find that a Perseid meteor with a given photometric mass could be at given height up to 1.5 magnitudes fainter than a Leonid meteor with the same mass. Therefore it needs additional time to reach the limiting magnitude of the camera and it is first detected at a lower altitude than the Leonid meteor. Light curves of the high-altitude Perseid meteors show that they become 1.5–2.0 magnitudes brighter about 15 to 20 km deeper in the atmosphere. Figure 3 shows that such a difference is indeed observed. The sputtering model thus successfully explains the different beginning heights of meteors with different initial velocities.

LIGHT CURVES OF METEORS

The light curve of the meteor represents its light production at different heights. It is constructed as a relationship of the meteor brightness to the height. The brightness of the meteor is determined for each frame by means of a calibration curve, which is determined using calibration stars. This apparent meteor brightness is recalculated to the 100 km distance of the event and called absolute brightness.

Fluctuations in the Sputtering Phase

Figure 4 shows typical light curves of the high-altitude meteors. Meteors 2000178, 2000179, 99173, and EN130801A are plotted. Only those parts of the meteor luminous trajectories above 130 km are shown. With the exception of meteor 99173, light curves are also available below this altitude. Note that the light curves cannot be described in traditional way using the F parameter. All meteors show an increase of brightness immediately the luminous trajectory starts. Usually such a hump covers several frames and then the brightness decreases again. Depression on the light curve could be up to one magnitude deep and several frames long. Because the meteor is usually faint at this part of its luminous trajectory, the signal-to-noise ratio is small. Nevertheless, the meteor brightness is determined with a precision of several tenths of magnitude. This means that the hump and following depression is a truly observed effect and not an error of measurement. A gradual increase of the brightness usually follows, but is not smooth. The meteor brightness typically fluctuates. The appearance of the meteors rapidly changes, too. They usually start as small diffuse objects that change shape from frame to frame, as described first by Spurný et al. (2000b). Vinkovic (Forthcoming) was able to successfully reproduce such appearance using the direct simulation Monte Carlo model. The sputtering and relative position between the camera and the meteor path is responsible for the changing appearance of the meteor shape. According to this model, collisions are concentrated at the centre of the diffuse structure, which is indeed observed. Popova et al. (Forthcoming) proved that the observed light curves are comparable with the sputtering model. Despite the fact that they took into account only first collisions and did not follow the collision cascade, they derived the meteor brightness, which is slightly lower than our data but roughly correspond to them.

The Beginning of the Ablation Phase

Around an altitude of 130 km, the meteor light curve starts to resemble the light curve of the standard meteors and could be characterized using traditional methods. We first tried to investigate at what altitudes this occurs. We define the beginning height of the ablation phase H_{BA} as the height at which the meteor brightness starts to steadily increase. Specifically, it is the point where the slope of the light curve changes significantly and it is followed by similar slopes on several consequent frames. It is demonstrated in Fig. 5 with meteor 20010467 (beginning height 148 km), a typical high-altitude meteor. The vertical dashed line indicates the above-defined height H_{BA} . Moreover, the standard meteors are represented in this plot by the light curve of meteor 20010209. Basic data on both meteors are provided in Table 3.

Table 3. Basic data on meteors. The table compares meteors 20010290 and 20010467 as representative of both groups of standard and high-altitude meteors.

	20010290	20010467
Date	18 November 2001	18 November 2001
Time (UT)	9:04:12	10:17:14
Photometric mass (g)	0.5×10^{-2}	1
Maximum brightness (mag)	0.2	-5.5
Parameter F	0.53	0.58
Beginning height (km)	117.2	148
Height of maximum brightness (km)	106.5	100.9
Terminal height (km)	97.6	91.7

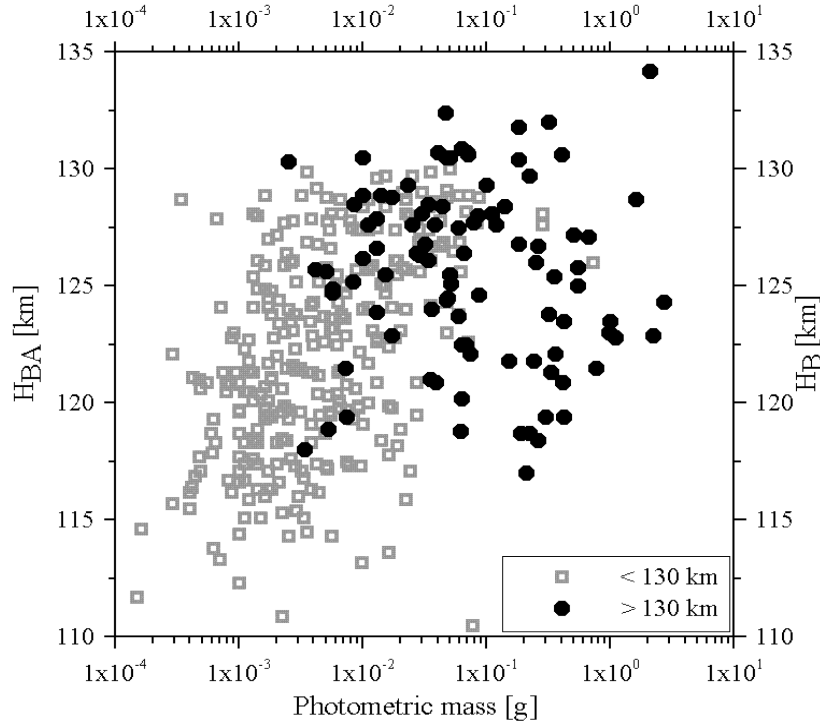


Fig. 6. The black dots represent the beginning height of the ablation phase H_{BA} of the high-altitude meteors, whereas the gray squares are the beginning heights of the standard meteors. All meteors belong to the 2001 Leonid meteor shower.

Figure 6 shows the H_{BA} of all high-altitude Leonid meteors for which it was possible to determine this value. For the majority of meteors, this height lies between 120 and 130 km and there is no relationship with the meteor photometric mass. We also investigated any possible effect of the different zenith distance of the radiant, but we found no influence. The value differs for each meteor regardless of the meteoroid mass and atmospheric trajectory slope. For comparison, the beginning heights of the standard meteors were included with this figure. The beginning heights of the standard meteors slowly increase with increasing photometric mass up to 130 km, but the spread of values for a given mass is again broad. Comparison with the high-altitude meteors proves that the choice of the altitude 130 km as the boundary between both groups of meteors was appropriate. If we take into account heights H_{BA} of the high-altitude meteors instead of their actual beginning height, we can recognize 132 km as

the real ceiling altitude. Above this altitude we see neither smooth light curve nor the classic appearance of the meteors. In our opinion, this altitude represents the boundary between two different processes, which are responsible for the light production of the meteors, i.e., sputtering above 130 km and ablation below this altitude.

Figure 7 provides another proof for this interpretation. The meteor brightness at the beginning height of the ablation phase M_{BA} as well as the maximum brightness M_{Max} of the meteor are plotted in relation to the meteor photometric mass. The dashed lines represent fits on both data sets. Brightness M_{BA} increase with increasing mass. If we assume that meteor reaches the brightness M_{BA} only due to sputtering, we should receive:

$$M_{BA} \sim -2.5 \log R_m^2 n_{atm} \sim -\frac{5}{3} \log m_p n_{atm} \quad (9)$$

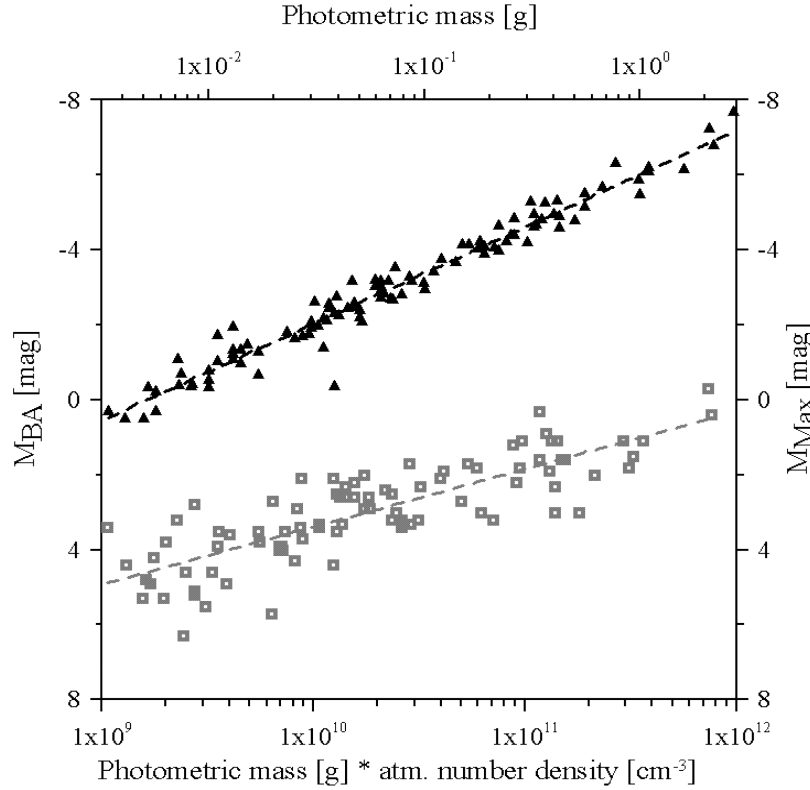


Fig. 7. This plot shows the brightness of the high-altitude meteors. The gray squares represent the meteor brightness at the beginning height of the ablation phase M_{BA} in relation to a product of the photometric mass and the number density of the atmosphere. The black triangles are the maximum brightness of the meteor M_{Max} as a function of the meteoroid photometric mass. Dashed lines are the logarithmic fits through both sets of data.

where R_m is the meteoroid radius, m_p is its photometric mass, and n_{atm} is the atmospheric number density at the altitude M_{BA} computed as the sum of number densities of O, O₂, and N₂ according to the MSIS-E-90 model of atmosphere (Hedin 1991). Actually, the slope of the fitted line is -1.54 , which is a value close to the theoretical one.

Below the altitude M_{BA} , the prevailing process is ablation. This means that the maximum brightness M_{Max} should be equal to $-2.5 \log m_p$. A perfect least square fit provides again a similar value of -2.65 . Thus the different slopes of both relationships are close to the theoretical values and provide us with additional evidence that sputtering and ablation are dominant processes for the radiation of the meteor above and below 130 km, respectively.

This result also agrees well with the sputtering model of Hill et al. (2004). They provide comparison of the meteor light curve produced when only thermal ablation is considered and when the sputtering and thermal ablation both contribute. It is clearly visible that the sputtering significantly contributes to the total meteor luminosity at higher altitudes.

The Ablation Phase

The light curves of the standard meteors could be characterized in different ways. The most traditional is a

parameter F , which represents the relative location of the point of the maximum brightness (e.g. Fleming et al. 1993; Murray et al. 1999; Koten et al. 2004; etc.). We can compute the parameter F as the average value from the individual $F_{\Delta M}$ values according to the equation (Fleming et al. 1993):

$$F_{\Delta M} = \frac{H_{B\Delta M} - H_{Max}}{H_{B\Delta M} - H_{E\Delta M}} \quad (10)$$

where $\Delta M = 0.25, 0.50, 0.75, \dots, 2.50, 2.75, 3.00$ and $H_{B\Delta M}$ and $H_{E\Delta M}$ are heights, where the meteor is by ΔM fainter than it is its maximum brightness M_{Max} . The parameter F is usually calculated as the mean value of all $F_{\Delta M}$. Light curves of 251 standard meteors are suitable for this calculation. They cover a broad range of values spreading between 0.2 and 0.89 as shown by the small gray crosses in Fig. 8. The mean value is 0.562 ± 0.041 . Standard meteors exhibit a broad variety of light curve shapes, which are nearly symmetrical on average, i.e., they reach the maximum brightness around the middle of the luminous trajectory.

The light curve of the high altitude meteors—as is the meteor 20010467 in Fig. 5—cannot be characterized by the same procedure because they usually display a difference of several magnitudes between the meteor brightness at the beginning height of the ablation phase and its brightness at the

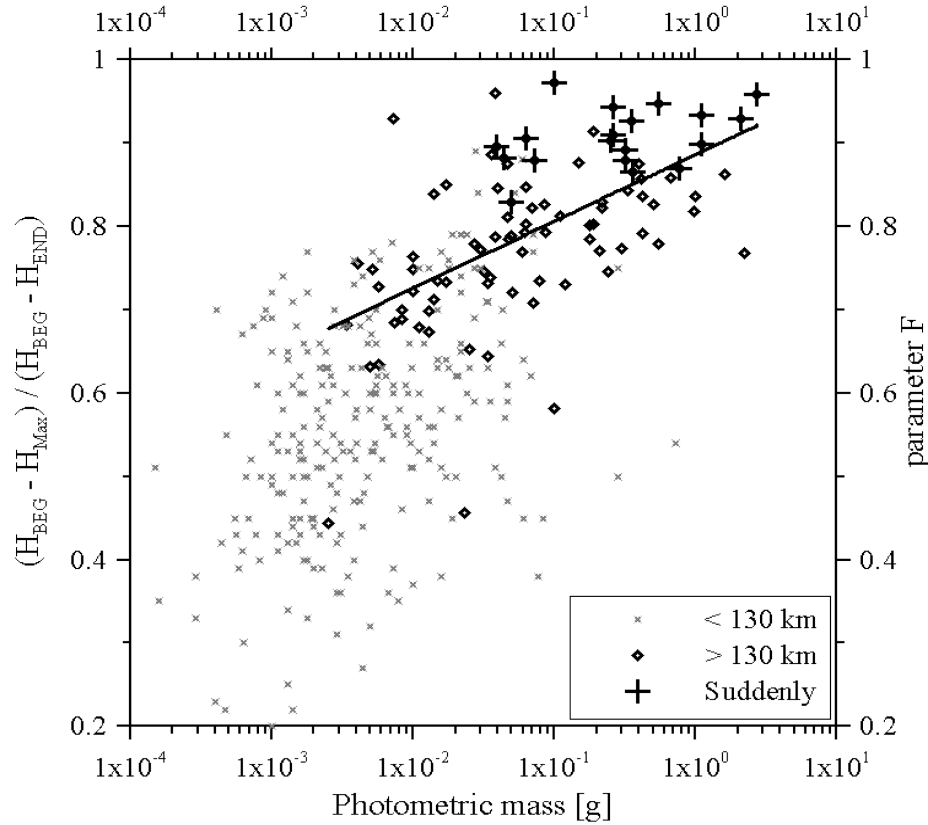


Fig. 8. The parameter F as a function of the photometric mass is given. Empty diamonds represent meteors above 130 km, the black line the logarithmic fit on them, and gray crosses standard meteors. 92 high-altitude meteors and 251 standard meteors are included in this plot, all belonging to the 2001 Leonid meteor shower. Larger black crosses stress the high altitude meteors, which produce suddenly terminating light curves.

terminal height. Therefore we decide to define the parameter F_H :

$$F_H = \frac{H_{BA} - H_{Max}}{H_{BA} - H_{END}} \quad (11)$$

that also shows the location of the maximum brightness but in a simpler way than the traditional $F_{\Delta M}$. Values of F_H for 92 high-altitude meteors are also shown in Fig. 8. The minimum value is 0.444, the maximum value is 0.97, and the mean is 0.796 ± 0.010 . Almost all light curves have $F_H > 0.5$. Although the standard meteors do not show any significant relationship between the meteor photometric mass and its parameter F , those high-altitude meteors do. The black line in Fig. 8 represents a good logarithmic fit, which shows that the value of F_H tends to be higher for larger meteoroids. The heaviest meteoroids produce meteors with light curves with the maximum brightness almost at the end of the luminous trajectory.

It was already reported in previous studies (Murray et al. 1999; Campbell et al. 2000; Koten et al. 2004) that brighter meteors produce light curves with the maximum brightness in the second part of their luminous trajectory and that the light curves of fainter meteors are symmetrical on average. Our data confirms those results and moreover prolongs them to

even higher photometric masses of the meteors, where this trend is even more significant. In terms of the dustball model (Hawkes et al. 1975), it means that fainter meteors are fragmented before the radiation starts, whereas for brighter meteors, the high-altitude fragmentation is not as important. They are more similar to the classical compact meteors or the fragment in the later part of the luminous trajectory.

Suddenly Terminated Light Curves

Among the high-altitude meteors, we can find a group of meteors whose luminous trajectories terminate very quickly (1 to 3 frames) after they reach the point of maximum brightness. They resemble type 3 light curves of Koschny et al. (2002). The descending branch of the light curve is almost missing as is shown in Fig. 9, where five such cases are presented. Altogether we found 19 such meteors; all of them are the Leonids. The shapes of their light curves are very similar to those seen in this plot. The value of parameter F_N lies between 0.8 and 1 as is shown in Fig. 8. The mean value of F_N is 0.906. If we define the difference $\Delta H_{MAX-END}$ between the height of maximum brightness H_{MAX} and terminal height H_{END} , the average difference is only 4.8 km. On the other hand, the vertical length of the ascending branch

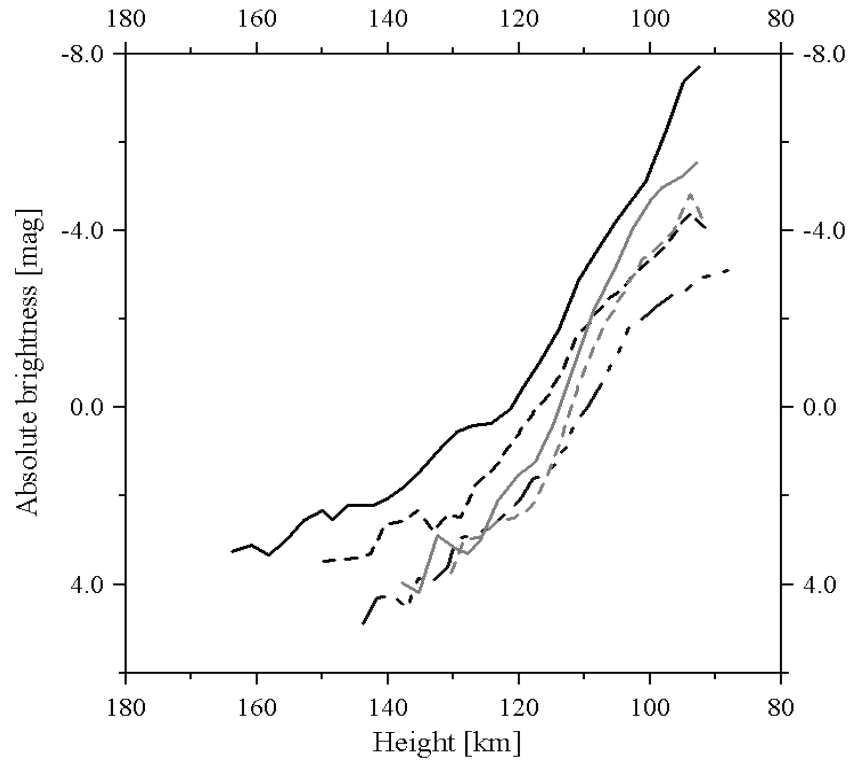


Fig. 9. This plot shows the light curves of five meteors, which are suddenly terminated after reaching maximum brightness. Note that all curves are complete and the whole luminous trajectory is covered. The meteors do not leave the camera's field of view. The descending branch of the light curve is simply missing or is very short.

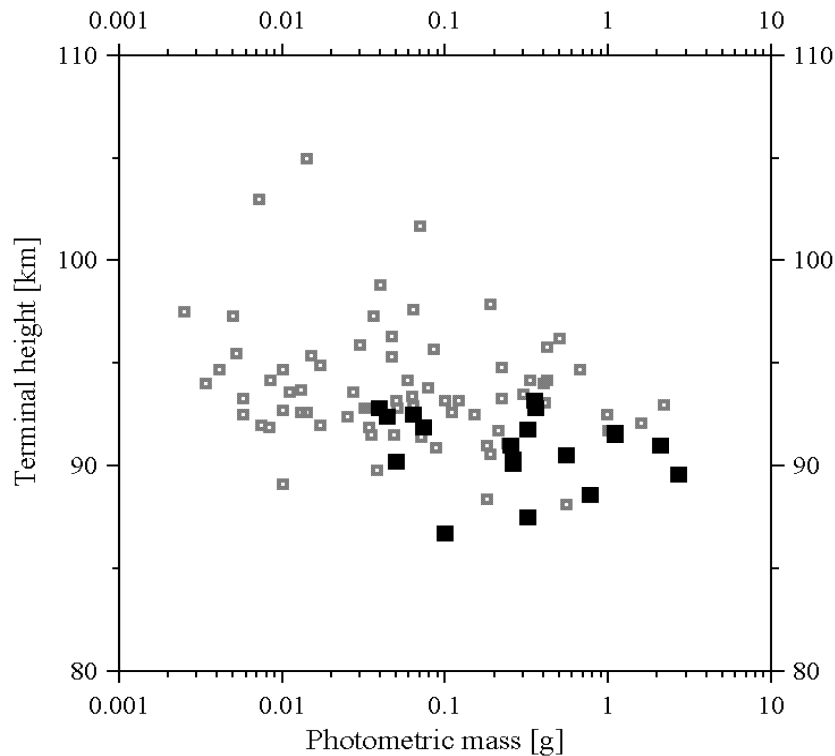


Fig. 10. The terminal height of the high-altitude meteors slightly decreases with increasing photometric mass. Meteors with suddenly terminated light curves (black squares) belong to the group whose terminal height is the lowest.

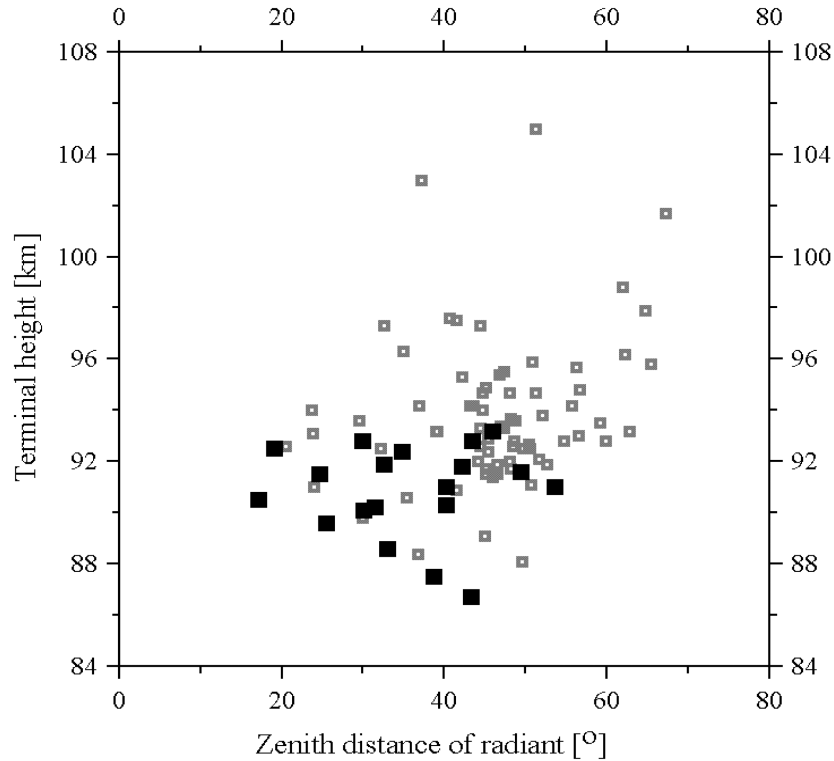


Fig. 11. Lower zenith distance of the radiant (i.e., steeper slope of the trajectory) is preferred among those meteors whose light curves terminate suddenly (black squares). Gray empty squares represent other high-altitude meteors observed during Leonid 2001 campaign.

$H_{\text{BEG}}-H_{\text{MAX}}$ is typically 40 or 50 km. We observe such behavior among meteors with a broad range of photometric mass between 3.9×10^{-2} and 2.7 g. Nevertheless, the higher masses are preferred, as shown by Fig. 10. We can see that among them in particular are meteors that penetrate deeper into the atmosphere in comparison with other meteors. The mean terminal height of these meteors is $H_{\text{END}} = 90.8 \pm 0.6$ km and their zenith distances between 15 and 55 degrees. This result is interesting in comparison with the findings of Spurný et al. (2000a). Working with a smaller sample of photographic Leonid meteors, they distinguished two typical shapes for the light curves. The second group of meteors was characterized by a very bright flare near the end of the luminous trajectory and its very steep final portion. Such light curves were found to be typical for the zenith distances $<45^\circ$. Our findings are similar. Suddenly terminated light curves are produced by meteors whose trajectories are steeper in the atmosphere. On the other hand, it seems this is not the only precondition. There are still many other meteors with a similar slope of the trajectory, whose light curves are not terminated quickly after the maximum brightness, as shown in Fig. 11. This phenomenon is probably caused by the combination of several circumstances and the steeper slope of the trajectory is only one of them. Another factor could be the composition of the meteoroid. Our idea is that the meteoroid is fragmented during its atmospheric passage into fragments of similar size and such fragments are depleted almost at the

same altitude. The result is the sudden end of the meteor luminosity. A similar scenario is suggested by Beech and Koten (2006). According to this paper, the descending branch of the meteor light curve is avoided because of the continuous fragmentation into smaller and smaller fragments, which eventually cannot produce any light.

PECULIAR METEORS

There are several meteors in our sample that deviate from the above-mentioned trends, having their beginning much higher than expected. Basic data on these meteors are given in Table 4. They include seven Leonids, one η -Aquarid, and one Lyrid. Special care was devoted to the measurement and the calculation of these meteors. The observed anomaly is not due to an obvious error in the method. The two most extreme cases are two Leonids observed only 33 seconds apart in 2000. Meteors 2000178 and 2000179 were first recorded at heights of 170 and 180 km, respectively. Unfortunately, the light curves of these meteors are incomplete. None of the video cameras used recorded the brightest part of the trajectory. Only bright flashes outside the field of view are visible on the tapes. The measurement of the photographic record of the meteor 2000178 shows that its maximum brightness is -2.9 ± 0.5 magnitudes, which implies a photometric mass of 0.1 g. According to Fig. 3, the beginning height of this meteor should be about 30 km lower. Due to

Table 4. Basic data on peculiar meteors having the beginning much higher than expected according to their photometric masses.

Meteor number	Date	Time (UT)	Beginning height (km)	Photometric mass ^a (g)	Shower
2000178	18 November 2000	3:29:34	170	0.1	Leo
2000179	18 November 2000	3:30:07	180	0.26–2.5 (E)	Leo
99173	18 November 1999	0:22:54	161	0.12–1.2 (E)	Leo
00502065	3 May 2000	1:54:23	150	0.025–0.22 (E)	η -Aqr
98011	16 November 1998	16:45:19	184	10 (S)	Leo
98043	16 November 1998	16:54:17	178	3 (S)	Leo
99420024	20 April 1998	23:27:29	137	10^{-3} (E)	Lyr
98387	17 November 1998	21:38:01	136	0.8×10^{-3}	Leo
2000024	16 November 2000	0:51:19	134	0.9×10^{-3}	Leo

^aE = estimated value; S = according to Spurný et al. (2000a).

saturation of the photographic record of the second meteor, it is impossible to measure its brightness, but we can say for certain that this meteor is significantly brighter than the first one. Thus meteor 2000179 seems not to differ significantly from some other cases recorded during the 1998 Leonid observations.

A comparison of both meteors shows that the height of maximum brightness and the terminal heights of the meteor 2000178 are relatively higher, which could suggest fragmentation of the meteoroid. Therefore we suspect that the high-altitude fragmentation could cause this anomaly. Smooth and symmetrical light curves of faint meteors indicate that smaller meteoroids fragment before the onset of radiation (Campbell-Brown and Jones 2003). Conversely, we already know that high-altitude fragmentation is less important for the bigger meteoroids. According to Fig. 8, the parameter F is usually higher than 0.7 for masses of 0.1 to 10 g is broad, which means that the meteoroids should be less susceptible to the high-altitude fragmentation. Unfortunately, we cannot measure the value of the parameter F for these meteors, because only the beginning portion of their light curves was recorded. Nevertheless, let us assume that their light curves are closer to symmetrical and that the meteoroids are the subjects of high altitude fragmentation. A large scatter of meteoroid characteristics such as H_{BEG} , H_{BA} , or F are shows us that the meteoroids are not uniform and we can assume the existence of such particles even among high altitude meteors.

Fragmentation into numbers of smaller particles increases the effective cross-section of the meteoroid, which is an important quantity for the sputtering from the meteoroid surface. Let us assume the fragmentation of a 10 g meteoroid into a number of small grains. Several papers have shown that a fundamental grain mass distribution is proportional to $m^{-\alpha}$, where α is the grain distribution index (Beech and Murray 2003; Campbell-Brown and Koschny 2004). Both of the most anomalous meteors were recorded on November 18, 2000, so we apply the value $\alpha = 1.88$, which was computed for the relevant peak of the 2000 Leonid meteor shower (Brown et al. 2002b). Beech and Murray (2003) set the fundamental

Table 5. The parameters of fragmentation. The table shows how the chosen parameters of the fragmentation influence the number of all fragments N and the difference ΔM between the brightness of the fragmented and non-fragmented meteoroids. This value is calculated according to Equation 8. Parameters m_{lower} and m_{upper} describe the range of masses of particular grains, which are distributed into B bins.

m_{bottom} (kg)	m_{upper} (kg)	B	N	ΔM
10^{-6}	10^{-4}	50	5000	+3.0
10^{-6}	10^{-4}	20	5300	+3.0
10^{-6}	10^{-4}	10	5900	+3.1
10^{-6}	10^{-3}	50	5000	+3.0
10^{-6}	10^{-3}	20	5500	+3.0
10^{-6}	10^{-3}	10	6400	+3.1
10^{-6}	10^{-2}	20	5800	+3.1
10^{-5}	10^{-3}	20	500	+2.2
10^{-5}	10^{-2}	20	550	+2.2
10^{-4}	10^{-2}	10	60	+1.3

grains limits $m_{\text{lower}} = 10^{-10}$ kg and $m_{\text{upper}} = m_{\text{total}}/2, 5$ or 10 , where m_{total} is the initial mass of the meteoroid. The fundamental grains are distributed in 10, 20 or 50 bins between m_{lower} and m_{upper} . Note that the meteors their light curves simulated were several orders smaller. We probably cannot assume that a 10 g meteoroid is also fragmented into fundamental grains. In such a case, we would receive a barely imaginable number of fragments ($\sim 10^7$). We therefore assume coarse fragmentation into larger fragments with the same bulk density as the original meteoroids. We adopt value 700 kg/m^3 , which Spurný et al. (2000a) computed for a Leonid fireball. We calculated the total cross-section of all fragments as well as the cross-section of the non-fragmented meteoroid of the same mass. Equation 8 provides us with the opportunity to compare the brightness of the meteors in both cases. We still assume the power law distribution with the mass distribution index α . The results for different sets of the parameters for the 10 g meteoroid are presented in Table 6. In relation to the chosen parameters, the non-fragmented

meteoroid is usually of 2 or 3 magnitudes fainter at the same height at which the meteoroid fragmented into a number of small grains. The typical light curves of the high-altitude meteors (Figs. 4 and 5) show that such a meteor needs approximately 20 to 30 km decrease in altitude to increase its brightness by up to 3 magnitudes, which is the difference between the observed and expected beginning height. Thus this approximate calculation shows that high-altitude fragmentation could explain the anomalously high beginning heights of some meteors.

CONCLUSIONS

Within all our observational programs, we detected 164 meteors with beginning heights above 130 km. Although the high-altitude meteors were also observed among other meteor showers, the Leonids account for the majority of such events, and beginning heights above 130 km are quite usual for them. On the other hand, beginning heights higher than 160 km are rare even for Leonid meteors.

We investigated the properties of the high-altitude meteors and found that they are in many aspects comparable with the results of the models that take sputtering from the meteoroid surface into account. The beginning height of the high-altitude meteors behave according to the model of Vinkovic (Forthcoming). In addition, the difference in the beginning height of the Leonids and the Perseids can be explained within this model. Observed light curves and the meteor shapes correspond to that modeled by Hill et al. (2004), Vinkovic (Forthcoming), and Popova et al. (Forthcoming). A comparison of the recorded data and sputtering models proves that the cascade of the collisions is sufficient to explain the radiation of meteors above 130 km. Around this altitude, it is probable that both processes contribute. For each meteor, we can find the point where the thermal ablation finally starts to dominate. This point usually lies between 120 and 130 km and its altitude is not related to the meteoroid mass. From the point of view of three phases of the high-altitude meteor radiation, which were distinguished by Spurný et al. (2000b), we can match the diffuse phase with the sputtering dominated region, the intermediate phase with the region where both processes contribute comparably, and finally the “sharp ablation” phase with the region of altitudes where the radiation is given solely by the meteor ablation.

We cannot omit also high-altitude fragmentation, the process of which is important especially for fainter meteors. Several peculiar meteors were observed, whose beginning heights are significantly higher than the beginning heights of other meteors with similar mass. According to their photometric masses, these meteoroids belong to the intermediate group between unambiguously fragmented smaller meteoroids and non-fragmented larger meteoroids. Assuming that significant high-altitude fragmentation of these cases could increase the effect of the sputtering from the

surfaces of individual fragments, we can explain their higher than expected beginning heights.

Acknowledgments—This study was supported by the Grant Agency of the Czech Republic, grant no. 205/02/P038. We would like to express our gratitude to the students who participated in the processing of the video tapes, especially on the measurement of the 2001 Leonid meteors records. The patient work of Pavel Macho, Jiří Pálek, Petr Zasche, Stanislav Podaný, Lukáš Shrbený, and Jitka Čermáková was very helpful. We thank also Mr. Aleš Kolář, who participated as the observer on the 1999 Leonid expedition. The authors would like to thank both referees, Peter Jenniskens and Noah Brosch, whose valuable comments significantly improved the first version of this paper.

Editorial Handling—Dr. Dina Prialnik

REFERENCES

- Beech M. and Murray I. S. 2003. Leonid meteor light-curve synthesis. *Monthly Notices of the Royal Astronomical Society* 345:696–704.
- Beech M. and Kotev P. 2006. Sudden ending Leonids: The inverse problem. *WGN* 34:55–57.
- Borovička J. and Jenniskens P. 2000. Time-resolved spectroscopy of a Leonid fireball afterglow. *Earth, Moon, and Planets* 82/83: 399–428.
- Brosch N., Schijvarg L. S., Podolak M., and Rosenkrantz M. R. 2001. Meteor observations from Israel. Proceedings, Meteoroids 2001 Conference. pp. 165–173.
- Brown P. G., Campbell M. D., Hawkes R. L., Treijsmeijer C., and Jones J. 2002a. Multi-station electro-optical observations of the 1999 Leonid meteor storm. *Planetary and Space Science* 50:45–55.
- Brown P., Campbell M., Suggs R., Cooke W., Theijsmeijer C., Hawkes R. L., Jones J., and Ellis K. J. 2002b. Video and radar observations of the 2000 Leonids: Evidence for a strong flux peak associated with 1932 ejecta? *Monthly Notices of the Royal Astronomical Society* 335:473–479.
- Campbell M. D., Brown P. G., LeBlanc A. G., Hawkes R. L., Jones J., Worden S. P., and Correll R. R. 2000. Image-intensified video results from the 1998 Leonid shower: I. Atmospheric trajectories and physical structure. *Meteoritics & Planetary Science* 35: 1259–1267.
- Campbell-Brown M. and Jones J. 2003. Determining the initial radius of meteor trains: Fragmentation. *Monthly Notices of the Royal Astronomical Society* 343:775–780.
- Campbell-Brown M. D. and Koschny D. 2004. Model of the ablation of faint meteors. *Astronomy & Astrophysics* 418:751–758.
- Cepelch Z. 1968. Discrete levels of meteor beginning height. Smithsonian Astrophysical Observatory Special Report #279. pp. 1–55.
- Cepelch Z. 1988. Earth's influx of different populations of sporadic meteoroids from photographic and television data. *Bulletin of the Astronomical Institute of Czechoslovakia* 39:221–236.
- Cook A. F. 1973. A working list of meteor streams. In *Evolutionary and physical properties of meteoroids*, edited by Hemenway C. L., Millman P. H., and Cook A. F. IAU Colloquium 13. Washington, D.C.: NASA. pp. 183–191.

- Gährken B. and Michelberger J. 2003. A bright, high-altitude 2002 Leonid. *WGN* 31:5–6.
- Hawkes R. L. and Jones J. 1975. A quantitative model for the ablation of dustball meteors. *Monthly Notices of the Royal Astronomical Society* 173:339–356.
- Hawkes R. L., Jones J., and Cepelch Z. 1984. The populations and orbits of double-station TV meteors. *Bulletin of the Astronomical Institute of Czechoslovakia* 35:46–64.
- Hedin A. E. 1991. Extension of the MSIS thermospheric model into the middle and lower atmosphere. *Journal of Geophysical Research* 96:1159–1172.
- Hill K. A., Rogers L. A., and Hawkes R. L. 2004. Sputtering and high altitude meteors. *Earth, Moon, and Planets* 95:403–412.
- Field D., May P. W., Pineau des Forêts G., and Flower D. R. 1997. Sputtering of the refractory cores of interstellar grains. *Monthly Notices of the Royal Astronomical Society* 285:839–846.
- Fleming F. E. B., Hawkes R. L., and Jones J. 1993. Light curves of faint television meteors. In *Meteoroids and their parent bodies*, edited by Štohl J. and Williams I. P. Bratislava, Slovakia: Astronomical Institute of the Slovak Academy of Sciences. p. 261.
- Fujiwara Y., Ueda M., Shiba Y., Sugimoto M., Kinoshita M., Shimoda C., and Nakamura T. 1998. Meteor luminosity at 160 km altitude from TV observations for bright Leonid meteors. *Geophysical Research Letters* 25:285–288.
- Jenniskens P. and Butow S. 1999. The 1998 Leonid multi-instrument aircraft campaign—An early review. *Meteoritics & Planetary Science* 34:933–943.
- Jenniskens P. and Rairden R. L. 2000. Buoyancy of the “Y2K” persistent train and the trajectory of the 04:00:29 UT Leonid fireball. *Earth, Moon, and Planets* 82/83:457–470.
- Koschny D., Reissaus P., Knöfel A., Trautner R., and Zender J. 2002. Modelling the fragmentation of meteoroids using Poisson statistics and application to the Leonids 2001. Proceedings, Asteroids, Comets, Meteors 2002 Conference. pp. 157–160.
- Koten P., Spurný P., Borovička J., and Štork R. 2001. Extreme beginning heights for non-Leonid meteors. Proceedings, Meteoroids 2001 Conference. pp. 119–122.
- Koten P. 2002. Software for processing of meteor video records. Proceedings, Meteoroids 2001 Conference. pp. 197–200.
- Koten P., Borovička J., Spurný P., Betlem H., and Evans S. 2004. Atmospheric trajectories and light curves of shower meteors. *Astronomy & Astrophysics* 428:683–690.
- LeBlanc A. G., Murray I. S., Hawkes R. L., Worden P., Campbell M. D., Brown P., Jenniskens P., Correll R. R., Montague T., and Babcock D. D. 2000. Evidence for transverse spread in Leonid meteors. *Monthly Notices of the Royal Astronomical Society* 313: L9–L13.
- Lindblad B. A., Neslušan L., Porubčan V., and Svoreň J. 2003. IAU meteor database of photographic orbits—Version 2003. *Earth, Moon, and Planets* 93:249–260.
- Molau S. 1999. The meteor detection software MetRec. Proceedings, Meteoroids 1998 Conference. pp. 131–134.
- Murray I. S., Hawkes R. L., and Jenniskens P. 1999. Airborne intensified charge-couple device observations of the 1998 Leonid shower. *Meteoritics & Planetary Science* 34:949–958.
- Popova O. P., Strelkov A. S., and Sidneva S. N. Forthcoming. Sputtering of fast meteoroids’ surface. *Advances in Space Research*, doi:10.1016/j.asr.2006.05.008.
- Rogers L. A., Hill K. A., and Hawkes R. L. 2005. Mass loss due to sputtering and thermal processes in meteoroid ablation. *Planetary and Space Science* 53:1341–1354.
- Sarma T. and Jones J. 1985. Double-station observations of 454 TV meteors. I. Trajectories. *Bulletin of the Astronomical Institute of Czechoslovakia* 36:9–24.
- Southworth R. B. and Hawkins G. S. 1963. Statistics of meteor streams. *Smithsonian Contributions to Astrophysics* 7:261.
- Spurný P., Betlem H., Van’t Leven J., and Jenniskens P. 2000a. Atmospheric behavior and extreme beginning heights of the thirteen brightest photographic Leonid meteors from the ground-based expedition to China. *Meteoritics & Planetary Science* 35: 243–249.
- Spurný P., Betlem H., Jobse K., Koten P., and Van’t Leven J. 2000b. New type of radiation of bright Leonid meteors above 130 km. *Meteoritics & Planetary Science* 35:1109–1115.
- Spurný P., Borovička J., and Koten P. 2004. Multi-instrument observations of bright meteors in the Czech Republic. *Earth, Moon, and Planets* 95:569–578.
- Ueda M. and Fujiwara Y. 1995. Television meteor radiant mapping. *Earth, Moon, and Planets* 68:585–603.
- Vinkovic D. Forthcoming. Thermalization of sputtered particles as the source of diffuse radiation from high-altitude meteors. *Advances in Space Research*, doi:10.1016/j.asr.2005.08.035.
- Woodworth S. C. and Hawkes R. L. 1996. Optical search for high meteors in hyperbolic orbits. In *Physics, Chemistry and dynamics of interplanetary dust*. San Francisco: Astronomical Society of the Pacific. pp. 83–86.